Integral control of collocated smart structures

Sumeet S. Aphale, Andrew J. Fleming, and S. O. Reza Moheimani

School of Electrical Engineering and Computer Science, University of Newcastle, Callaghan, NSW, Australia;

ABSTRACT

This paper introduces a simple and robust technique for vibration control in smart structures with collocated sensors and actuators. The technique is called Integral Resonant Control (IRC). We show that by adding a direct feed-through to a collocated system, the transfer function can be modified from containing resonant poles followed by interlaced zeros, to zeros followed by interlaced poles. This structure permits the direct application of integral feedback and results in good stability and damping performance. To alleviate the problems due to unnecessarily high controller gain below the first mode, a slightly complicated second-order controller is also discussed. A piezoelectric laminate cantilever beam used to test the proposed control scheme exhibits up to 24 dB modal damping over the first eight modes.

Keywords: Piezoelectric transducers, collocated sensor-actuator pairs, vibration damping, IRC

1. INTRODUCTION

Noise and vibration is of significant concern in many industrial, scientific and defense applications.[1–3] Structures with integrated sensors and actuators, also known as *smart structures*, have shown to offer improved vibration control in applications where passive techniques are either insufficient or impractical. Selection and integration of actuators and sensors, and the control system design are the two significant design tasks in active structural control. In this work a new control methodology is introduced for the most common class of smart structures with integrated piezoelectric actuators and sensors. Piezoelectric sensors and actuators have been the transducer of choice for smart structures due to their small volume, low weight and ease of structural integration, see[4–7] for an introduction to the use of piezoelectric transducers in structural actuation and sensing.

Variable resonance frequencies, high system order and highly resonant dynamics are some of the foremost difficulties associated with the control of flexible structures. Traditional control system design techniques such as LQG, H_2 and H_∞ commonly appear in research works and have been well documented.[8–11] Unfortunately, the direct application of such techniques may result in control systems of high-order and unacceptable stability margins.

Robust performance, more damping, and ease of implementation are the main advantages that the controllers based on the underlying structure of a collocated resonant mechanical system have proven to offer, relative to traditional techniques. The interlacing of poles and zeros up the $j\omega$ axis is the most useful characteristic of a collocated system. This results in a phase response that lies continuously between 0 and -180 degrees. Positive Position Feedback (PPF)[12] exploits this property and results in controllers that are stable in the presence of uncontrolled in-bandwidth modes. Their quick roll off characteristics at higher frequencies reduce the risk of destabilizing systems with high-frequency dynamics. However, PPF controllers are also equal in order to the system that they are designed to control and require non-linear search based models for their design process. They are also difficult to tune if more than one mode is to be controlled. Velocity feedback[13] is another technique that exploits the known phase response of collocated systems. Velocity feedback implements pure viscous damping with a phase margin of 90 degrees. Unfortunately, the high frequency gain must be attenuated to avoid noise amplification and destabilization due to unmodeled or non-collocated dynamics. Although velocity feedback has been applied in practice, the two additional poles required at high frequencies while implementing this technique result in poor phase margin. Resonant control is another approach that has been successfully applied to collocated resonant systems.[14] A resonant controller guarantees closed-loop stability in the presence

Further author information: (Send correspondence to S. O. Reza Moheimani)
S. O. Reza Moheimani: E-mail: Reza.Moheimani@newcastle.edu.au, Telephone: 61 2 492 16030

Active and Passive Smart Structures and Integrated Systems 2007, edited by Yuji Matsuzaki, Mehdi Ahmadian, Donald Leo,
Proc. of SPIE Vol. 6525, 652521, (2007) · 0277-786X/07/$18 · doi: 10.1117/12.715477

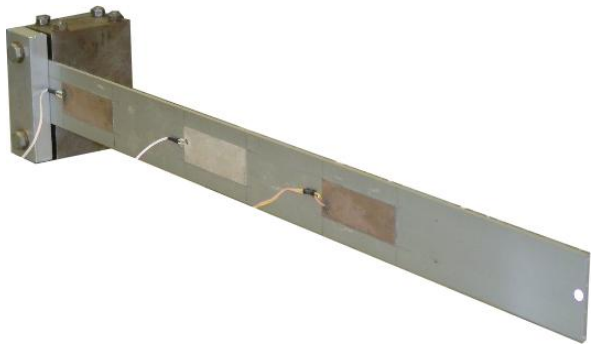

Figure 1. Picture of the cantilever beam.

of uncontrolled out-of-band modes of the structure but the high-pass nature of the controller, may not be suitable in certain applications.

This paper proposes a control design based on augmenting the feed-through of a collocated system; that is, to add a small portion of the actuator signal to the sensor signal. Section 3 shows that this procedure results in the addition of a pair of resonant system zeros at an arbitrary frequency. Choosing this frequency lower than the first mode results in a compound system with interlaced zeros then poles, rather than poles then zeros. The phase response of this system lies between 0 and -180 degrees. This property can be exploited through the use of direct integral feedback which results in a loop phase response that lies between -90 and +90 degrees, i.e., has a phase margin of 90 degrees and infinite gain margin. Integral Resonant Control, IRC, is shown to substantially damp multiple resonant modes.

The following section presents the objectives and scope of this work together with a description of the experimental apparatus. The characteristics of collocated systems, feed-though augmentation, and IRC design are then discussed in Section 3. Experimental results demonstrating up to 24 dB reduction over eight modes and conclusions follow in Sections 4 and 5.

2. OBJECTIVES

The main objective of this work is to investigate the pole-zero interlacing exhibited by transfer functions of certain collocated resonant mechanical systems and use this property to damp the low-frequency resonant modes of the system. A mathematical proof for the pole-zero interlacing phenomenon in transfer functions of certain collocated resonant mechanical systems will be given. It will be shown that by adding a specific feed-through term to this transfer function, the implementation of simple second-order controllers that damp vibrations over multiple low-frequency resonant modes is possible. The appropriate feed-through term is identified in a parametric form. A cantilever beam is a typical example of a resonant mechanical system and is susceptible to high amplitude vibrations when disturbed. The proposed algorithm will be experimentally validated on a cantilever beam.

2.1. Experimental setup

The experimental setup used in this work is shown Figure 1. This cantilever beam has three pairs of collocated piezoelectric patches attached to it of which, one collocated pair is used for actuation and sensing, one collocated pair is shorted and of the third collocated pair, one patch is shorted and the other is used as an independent disturbance source. Note that the shorted piezoelectric patches have no effect on the open- or closed-loop beam dynamics whatsoever.

Figure 2 shows the resultant two-input two-output cantilever beam system, where the inputs are the control voltage applied to the collocated actuator patch (u) and the disturbance generated by the third (non-collocated) piezo-patch (w) and the outputs are the collocated sensor voltage (y) and the tip displacement (z). A Polytec scanning laser vibrometer (PSV-300) was used to measure the frequency response function (FRF). The measured FRF $G_{ij}(\mathrm{j}\omega)$ is a 2×2 matrix where each element $G_{ij}(\mathrm{j}\omega)$, $i, j = 1$ and 2, corresponds to a particular combination

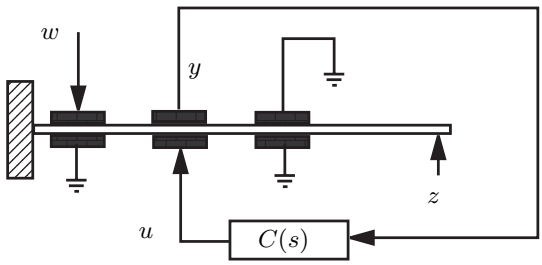

Figure 2. Schematic diagram of the control strategy showing the inputs and outputs.

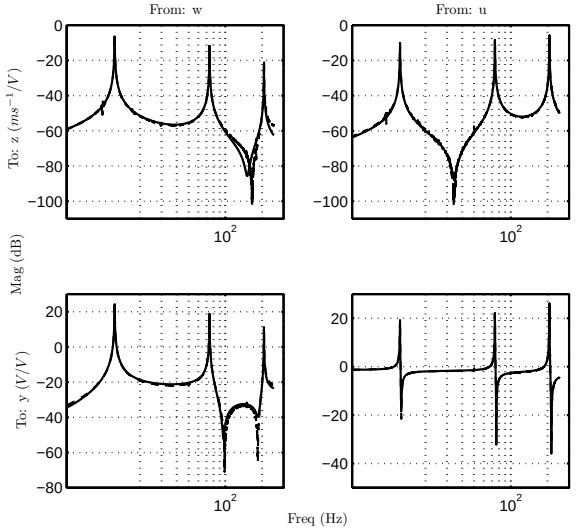

Figure 3. Magnitude response in dB of the measured (- -) and modeled (—) system.

of the input and output (for example $G_{yw}(\mathrm{j}\omega) = y(\mathrm{j}\omega)/w(\mathrm{j}\omega)$ when $u = 0$). These FRFs are determined by applying a sinusoidal chirp (from 5 - 250 Hz) as input (w and u) to the corresponding piezoelectric actuator and measuring the output signals (y and z). The frequency range is chosen such that it captures the first three resonant modes of the cantilever beam.

3. CONTROLLER DESIGN

An accurate system model is required for the purpose of analysis and control design, that was procured using a subspace based modeling technique.[15] The magnitude and phase responses of the model and experimental system are shown in Figures 3 and 4. As can be seen, the obtained model captures the dynamics of the system accurately.

3.1. Properties of collocated transfer functions

Many interesting properties are displayed by the trasnfer function associated with a single collocated actuator/sensor.[16,17] The property of interest on which this work is based is the interlacing of resonant poles and zeros. As a result, the phase of a collocated transfer function lies between $0°$ and $-180°$. The system transfer

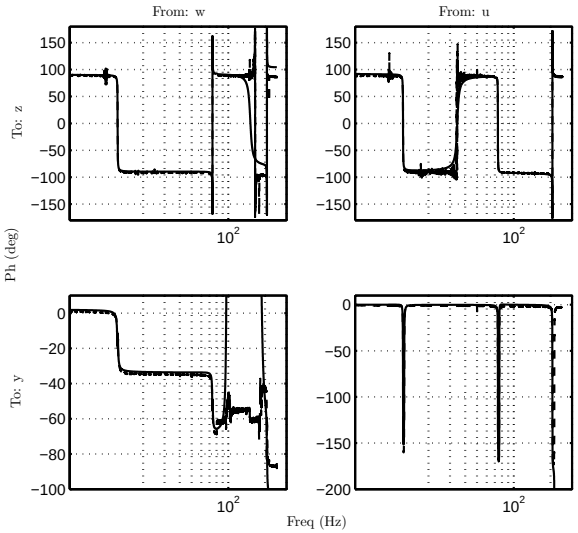

Figure 4. Phase response of the measured (- -) and modeled (—) system.

function can be represented as the sum of many second order blocks and can be written as

$$G(s) = \sum_{i=1}^{M} \frac{\alpha_i}{s^2 + 2\zeta_i\omega_i s + \omega_i^2} \tag{1}$$

where $\alpha_i > 0 \quad \forall i$ and $M \to \infty$.[18] For all practical applications a very large but finite M represents the number of modes that sufficiently describe the elastic properties of the structure under excitation. It is common practice to identify a bandwidth of interest and control resonant modes that lie within that bandwidth. In such scenarios, the first $N < M$ (in-band) modes are controlled while the remaining $N + 1$ and above (out-band) modes are left uncontrolled. A truncated model of the system that includes only those modes which are to be controlled is used. Significant errors are introduced as a result of this truncation, as the in-bandwidth zeros of the system are highly dependent on the out-of-bandwidth poles. Hence, when the model is truncated, the in-bandwidth zero dynamics are significantly perturbed. To account for these perturbations an appropriate feed-through term is added to the truncated system model. It has been shown that a constant feed-through is sufficient to model the effect of high frequency modes on low frequency zeros.[19] The truncated system can be written as,

$$\tilde{G}(s) = \sum_{i=1}^{N} \frac{\alpha_i}{s^2 + 2\zeta_i\omega_i s + \omega_i^2} + D \tag{2}$$

such that $D \in \mathbb{R}$. Note that the collocated beam transfer function $G_{yu}(s)$ is of the form (2).

3.2. Pole-zero interlacing and feed-through

A mathematical derivation and explaination of the interlacing pole-zero pattern exhibited by the collocated transfer function $G_{yu}(s)$ will be given in this section. The choice of a particulat feed-through D, and its effect, will also be elaborated. For the sake of brevity , zero damping is assumed ($\zeta = 0$). However, the results can easily be extended to systems with damping. The first theorem shows that a system obtained by adding N second order sections of the form $\frac{\alpha_i}{s^2+\omega_i^2}$ has N pairs or complex conjugate poles and $N - 1$ pairs of complex conjugate zeros such that between every two poles, there is a zero. The next theorem shows that for a system obtained by adding N second order sections of the form $\frac{\alpha_i}{s^2+\omega_i^2}$, the addition of a feed-through term $D \in \mathbb{R}$ can introduce a pair of complex conjugate zeros. Their proofs will appear in the full (Journal) version of this paper.

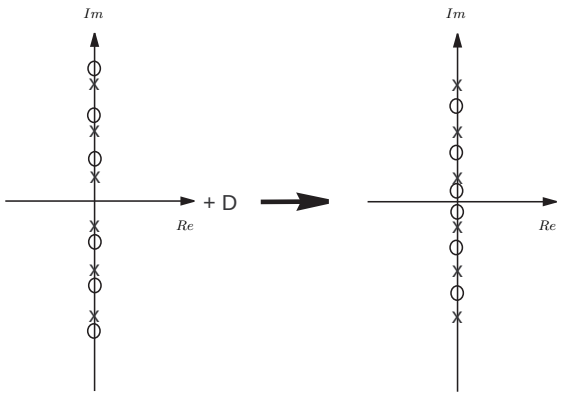

Figure 5. Poles (x) and Zeros (o) of the collocated transfer function, before and after the addition of the feed-through term (D).

THEOREM 3.1. *Let* $G(s) = \sum_{i=1}^{N} \frac{\alpha_i}{s^2+\omega_i^2}$ *such that* $\alpha_i > 0$ *for* $i = 1, 2, 3, \cdots$ *and* $\omega_1 < \omega_2 < \cdots < \omega_N$. *Then, between every two consecutive poles of* $G(s)$ *there exists a zero.*

THEOREM 3.2. *Let* $G(s) = \sum_{i=1}^{N} \frac{\alpha_i}{s^2+\omega_i^2}$ *such that* $\alpha_i > 0 \quad \forall i$ *and* $\omega_1 < \omega_2 < \cdots < \omega_N$. *If* $\tilde{G}(s) = G(s) + D$ *where* $D \in \mathbb{R}$ *and* $\tilde{G}(j\omega_z) = 0$ *such that* ω_z *is not a zero of* $G(s)$ *then,* $\tilde{G}(s)$ *can be written as* $\tilde{G}(s) = (s^2+\omega_z^2)\sum_{i=1}^{N} \frac{\beta_i}{s^2+\omega_i^2}$.

Figure 5 shows a typical pole-zero plot of the collocated transfer function, before and after addition of the feed-through term D. Note that the pole locations remain the same even after adding the feed-through term. The collocated transfer function of the cantilever beam used in the experiments is:

$$G_{yu}(s) = \frac{225}{s^2+0.3854s+6035} + \frac{8971}{s^2+1.49s+217100} + \frac{90960}{s^2+3.573s+1.697\times10^6} + 0.7456.$$

This fixed structure form can be obtained approximately by using the *residue* function in MATLAB from the identified collocated model $G_{yu}(s)$ in Figures 3 and 4. Due to the fully parameterized nature of the identified model, the residuals of each second order section will also contain a small 's' term that can be neglected. Note that in this case, $G_{yu}(s) \equiv \tilde{G}(s)$ (defined in Theorem 3.2), where

$$G(s) = \frac{225}{s^2+0.3854s+6035} + \frac{8971}{s^2+1.49s+217100} + \frac{90960}{s^2+3.573s+1.697\times10^6}, \text{ and}$$

$$D_1 = 0.7456.$$

The first resonant mode occurs at 12.33 Hz. Theorem 3.2 is used to find an arbitrary feed-through term $D_2 = -0.1372$ that places a zero at 4.1858Hz ($<$ 12.33 Hz). Thus, to account for D_1 and D_2, a feed-through term of $D_f = (-0.1372 - 0.7456) = -0.8828$, was added to $G_{yu}(s)$.

As Theorem 3.2 explains, the addition of a low-frequency zero results in a phase inversion at DC relative to the original transfer function. The magnitude and phase response of the collocated open-loop and modified transfer functions, $G_{yu}(s)$ and $(G_{yu}(s)+D_f)$ respectively, are plotted in Figure 7. It is observed is that the phase of the modified transfer function lies between 0 and -180 degrees; thus, a negative integral controller ($C(s) = \frac{-1}{s}$)

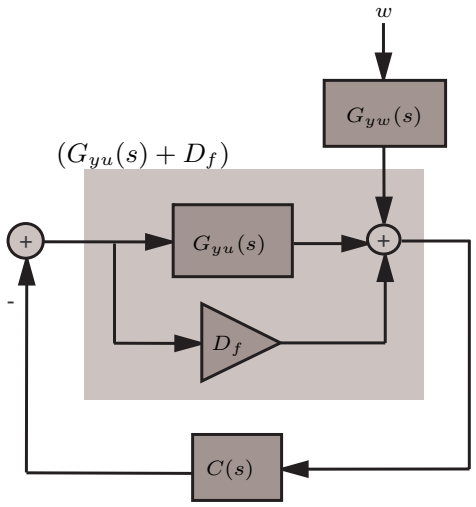

Figure 6. Schematic diagram of the implemented control strategy.

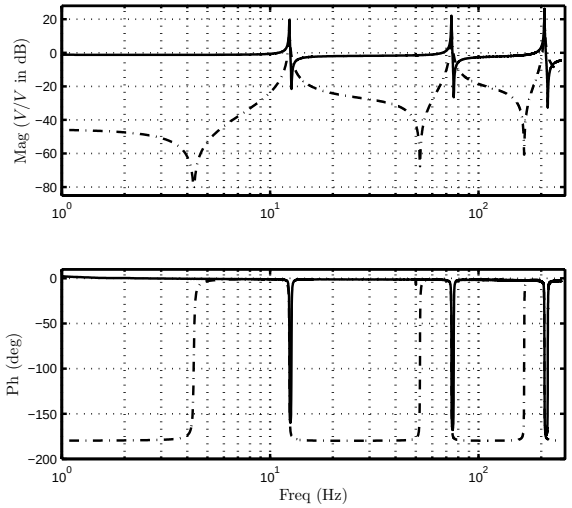

Figure 7. Open-loop collocated beam transfer function $G_{yu}(s)$ (—) and modified transfer function $(G_{yu}(s) + D_f)$ (- -).

in negative feedback, which adds a constant phase *lead* of 90 degrees will yield a loop transfer function whose phase response lies between +90 and -90 degrees, that is, the closed-loop system has a highly desirable phase margin of 90 degrees. In the following section, a simple integral controller, a lossy integral controller and a simple second-order band-pass filter type controller are discusses. A gain selection technique based on the root-locus plot is presented in Subsection 3.4.

3.3. Integral Resonant Control

The block diagram of the proposed Integral Resonant Control, IRC, scheme is shown in Figure 6. In the following discussion, three suitable controllers - direct integral control, its lossy variant and a simple band-pass filter type

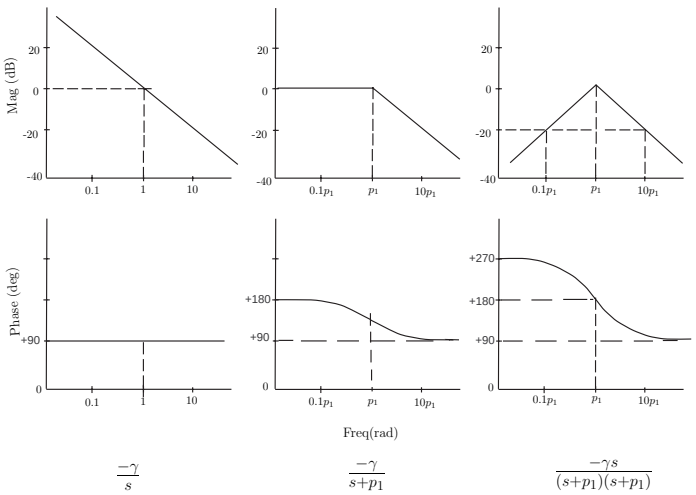

Figure 8. Typical bode plots of the three possible controllers assuming $\gamma = 1$

controller - are introduced and evaluated for performance and robustness. The frequency response of each controller is plotted in Figure 8. Selection of the controller gain $\gamma > 0$, will be discussed in Subsection 3.4.

- **Simple Integrator** $C(s) = \frac{-\gamma}{s}$: Integral control has been extensively researched and documented.[17] The main drawback in its application is the unnecessarily high gain imposed at low frequencies. This high control input at low frequencies may lead to actuator saturation.
- **Lossy integrator** $C(s) = \frac{-\gamma}{s+p_1}$: This controller has reduced gain at low frequencies. To effectively reduce low-frequency gain, it is necessary to select p_1 close to the first structural resonance frequency. The penalty associated with its implementation is of slightly reduced closed-loop phase margin.
- **Band-pass filter** $C(s) = \frac{-\gamma s}{(s+p_1)(s+p_1)}$: To ensure the controller response rolls-off at low-frequencies, a controller with two poles at p_1 $rad.s^{-1}$ and a zero at 0 $rad.s^{-1}$ is suitable. The resulting closed-loop phase margin is inferior to that exhibited by the two previous controllers but the gain attenuation is greater. The phase margin can be further improved by implementing $C(s) = \frac{-\gamma s}{(s+p_1)(s+p_2)}$ where $p_2 < p_1$.

3.4. Gain selection

The gain of the IRC, γ, can be determined by analyzing the loop gain. A root-locus plot depicts the trajectories traveled by the poles with respect to increase in the system gain, see Figure 9. It is found that by increasing the controller gain, the poles follow a curve and finally reach the zeros they are paired with. This plot also reveals the damping of each pole along the trajectory. As the gain increases, the poles initially move away from the imaginary axis and the damping increases until it reaches a maximum point. Further increases in gain drag the pole closer to the imaginary axis and reduce the damping. Finally the pole is placed at the same position as its paired zero. At this position, the improvement in damping is negligible.

Thus, the gain of the controller can be chosen such that maximal damping performance is achieved at the in-band resonant modes that lie within the bandwidth of interest. To achieve maximum damping of higher frequency modes, higher gains are required. This high gain may place the low frequency poles close to the imaginary axis (with no significant increase in damping) and thus low frequency modes are not attenuated. As we are considering a cantilever beam with dominant low frequency dynamics (with the first resonant mode at 12.33 Hz), a gain is chosen that provides optimal damping of the first three structural modes. For the system used in our experiments, the required gain was found to be $\gamma = 550$.

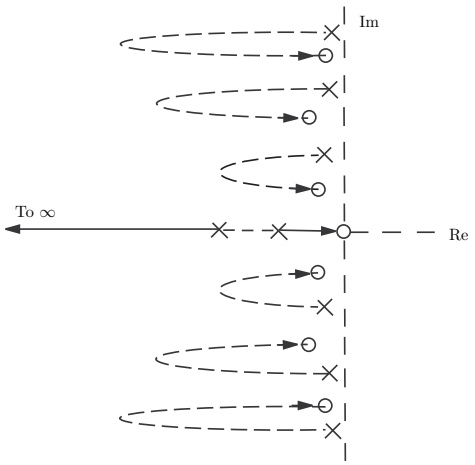

Figure 9. Root-Locus plot showing the trajectories of the poles due to change in system gain.

3.5. Summary

The IRC controller design process can be summarized in the following steps:

- **Step 1:** Measure the open- loop frequency response of the system and preferably obtain a model for the system as described in subsection 3.1.
- **Step 2:** Use results in Subsection 3.2. Determine the required feed-through term that adds a zero at a frequency lower than the first resonant mode of the system.
- **Step 3:** Design a controller of the form $C(s) = \frac{-\gamma s}{(s+p_1)(s+p_1)}$ by choosing p_1 to be approximately a decade lower in frequency than the first mode, see subsection 3.3.
- **Step 4:** By plotting the root-locus, select a suitable gain which results in peak attenuation at resonant frequencies lying in the band of interest, see subsection 3.4.
- **Step 5:** Implement IRC using either an analog or digital transfer function. Measure the open- and closed-loop frequency responses and check that they agree with the simulated results as shown in Section 4.

4. EXPERIMENTAL RESULTS

The controller was implemented digitally using a dSPACE rapid prototyping system with a sampling frequency of 20 KHz. The continuous transfer function of the controller is given by $C(s) = \frac{-550s}{(s+0.3(2\pi))(s+0.3(2\pi))}$. For a digital implementation, this was converted to a discrete transfer function using the zero order hold approximation. A time advance of one sample was incorporated into the control loop to account for the system delay. This is achieved by multiplying the transfer function of the controller by the forward shift operator z. This is possible because $C(z)$ is strictly proper and has a relative degree of 1. Frequency responses are measured from the input disturbance w to the output tip displacement z of the cantilever beam, denoted by G_{zw}. Simulated open- and closed-loop frequency responses are shown in Figure 10 (a). Measured open- and closed-loop frequency responses are shown in Figure 10 (b). The first three modes are attenuated by 22 dB, 24 dB and 21 dB respectively.

Open- and closed-loop frequency responses are measured for a band of frequencies from 0 Hz to 2.5 KHz, to evaluate the controller performance, see Figure 11. This band captures the first eight resonant modes of the cantilever beam. Table 1 shows the attenuation achieved for the first eight modes. The minimal attenuation of the fourth mode is due to the position of the collocated patches.

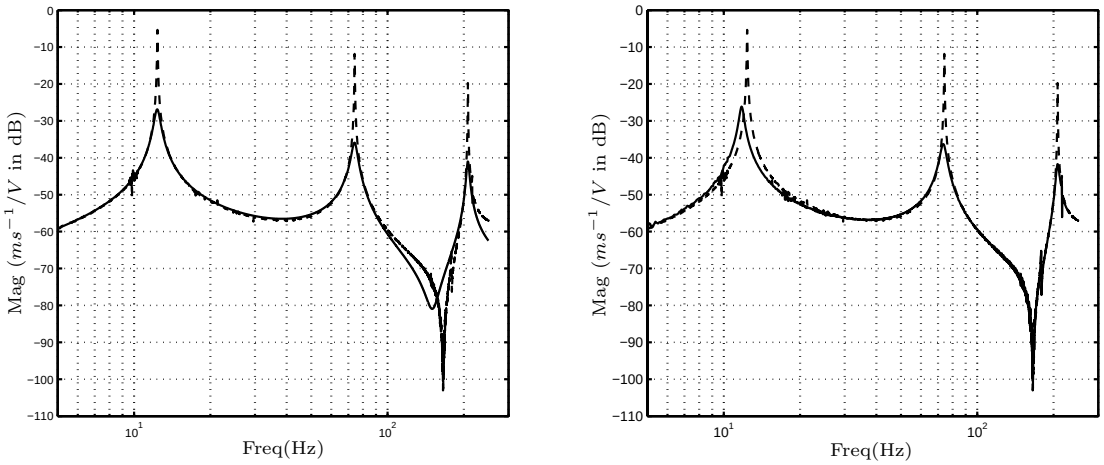

Figure 10. Simulated (a) and experimental (b) open-loop (- -) and closed-loop (–) responses of the cantilever beam measured from disturbance input w to the tip displacement z.

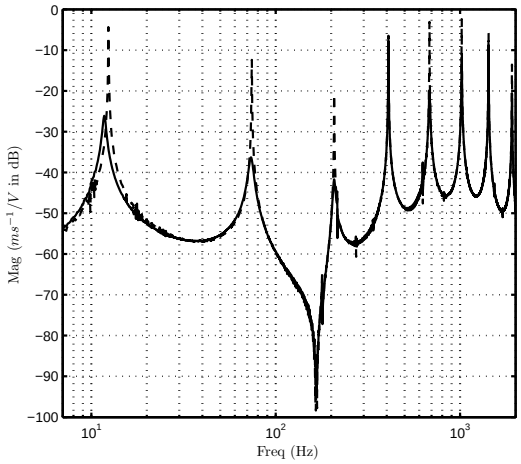

Figure 11. Open- (- -) and closed-loop (—) system response for the first eight modes of the cantilever beam measured from disturbance input w to the tip displacement z.

The robustness in performance of the IRC to variations in resonance frequencies is evaluated by first loading the cantilever beam with a mass and then recording its open- and closed-loop responses. The addition of mass changes the resonance frequencies and is equivalent to adding uncertainty. It is seen that even though the addition of mass shifts the resonant modes by as much as ten percent, there is minimal performance degradation. All of the eight modes show significant damping even with the mass present, see Figure 12. Table 2 documents the damping achieved on the loaded beam for the first eight modes.

Table 1. Damping for the first eight modes of the cantilever beam

Mode Number	1	2	3	4	5	6	7	8
Frequency(Hz)	12.33	74.25	207.48	408.75	682.32	1020.85	1427.23	1914.01
Attenuation (dB)	22	24	21	0.7	16	9	3	7

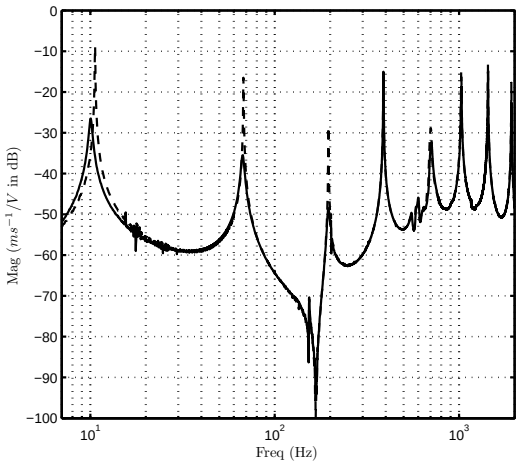

Figure 12. Open- (- -) and closed-loop (—) system response for the additional mass-loaded cantilever beam measured from disturbance input w to the tip displacement z.

5. CONCLUSIONS

The pole-zero structure found in the transfer functions of collocated smart structures is mathematically formulated. It is shown that adding a feed-through term to this system introduces a new pair of resonant zeros. A parametrized structure of the feed-through term in terms of frequencies at which it adds the resonant zeros is given. The phase response of the transfer functions of collocated smart structures show that by adding a pair of zeros at a frequency below the first resonant mode, a simple first- or second-order controller can provide good damping performance and stability margins. Three controllers motivated by the integral controller, are discussed for their performance benifits and drawbacks. The so-called Integral Resonant Control scheme, IRC, implemented on a cantilever beam is shown to damp the first eight resonant modes by up to 24 dB even under resonance frequency uncertainties.

6. ACKNOWLEDGMENT

This research was supported by the Australian Research Council and the ARC Center for Complex Dynamic Systems and Control.

REFERENCES

1. S. Salapaka, A. Sebastian, J. P. Clevland, and M. V. Salapaka, "Design identification and control of a fast nanopositioning device," in *Proc. American Control Conference*, pp. 1966 – 1971, May 2002.
2. L. Vaillon and C. Philippe, "Passive and active microvibration control for very high pointing accuracy space systems.," *Smart Materials and Structures* **8**, pp. 719–728, December 1999.
3. S. Wu, T. L. Turner, and S. A. Rizzi, "Piezoelectric shunt vibration damping of an F-15 panel under high-acoustic excitation," in *Proc. SPIE Smart Structures and Materials: Damping and Isolation*, **3989**, pp. 276 – 287, 2000.

Table 2. Damping for the first eight modes for a cantilever beam with added mass

Mode Number	1	2	3	4	5	6	7	8
Frequency(Hz)	10.625	67.48	195.76	356.68	702.38	1028.98	1435.82	1921.97
Attenuation(dB)	17	19	20	0.5	4	4	1	5

4. E. F. Crawley and J. de Luis, "Use of piezoelectric actuators as elements of intelligent structures," *AIAA Journal* **25**(10), pp. 1373–1385, 1987.
5. B. T. Wang and C. C. Wang, "Feasibility analysis of using piezoceramic transducers for cantilever beam modal testing," *Smart Materials and Structures* **6**(1), pp. 106–116, 1997.
6. C. R. Fuller, S. J. Elliott, and P. A. Nelson, *Active Control of Vibration*, Academic Press, 1996.
7. S. O. R. Moheimani and A. J. Fleming, *Piezoelectric transducers for vibration control and damping*, Springer-Verlag, 2006.
8. I. R. Petersen and H. R. Pota, "Minimax LQG optimal control of a flexible beam," *Control Engineering Practice* **11**, pp. 1273–1287, November 2003.
9. B. M. Chen, T. H. Lee, H. Chang-Chieh, Y. Guo, and S. Weerasooriya, "An H_∞ almost disturbance decoupling robust controller design for a piezoelectric bimorph actuator with hysteresis," *IEEE Transactions on Control Systems Technology* **7**, pp. 160–174, February 1999.
10. D. Halim and S. O. R. Moheimani, "Experimental implementation of spatial H_∞ control on a piezoelectric laminate beam.," *IEEE/ASME Transactions on Mechatronics* **4**, pp. 346 – 356, September 2002.
11. D. Halim and S. O. R. Moheimani, "Spatial H_2 control of a piezoelectric laminate beam: Experimental implementation.," *IEEE Transactions on Control Systems Technology* **10**, pp. 533 – 546, July 2002.
12. J. L. Fanson and T. K. Caughey, "Positive position feedback-control for large space structures," *AIAA Journal* **28**, pp. 717–724, April 1990.
13. C. W. de Silva, *Vibration Fundamentals and Practice*, CRC Press, 1999.
14. H. R. Pota, S. O. R. Moheimani, and M. Smith., "Resonant controllers for smart structures," *Smart Materials and Structures* **11(1)**, pp. 1 – 8, February 2002.
15. T. McKelvey, H. Akcay, and L. Ljung, "Subspace based multivariable system identification from frequency response data," *IEEE Transactions on Automatic Control* **41**, pp. 960–978, July 1996.
16. G. D. Martin, *On the control of flexible mechanical systems*. PhD thesis, Stanford University, U.S.A., 1978.
17. A. Preumont, *Vibration Control of Active Structures: An Introduction*, Kluwer, 1997.
18. P. C. Hughes, "Space structure vibration modes: how many exist? which ones are important?," *IEEE Control Systems Magazine* **8**, pp. 22–28, February 1987.
19. R. L. Clark, "Accounting for out-of-bandwidth modes in the assumed modes approach: implications on collocated output feedback control," *Transactions ASME Journal of Dynamic Systems Measurement and Control* **119**, pp. 390–395, 1997.